Received: 27 May 2018 | Revised and accepted: 1 October 2018

DOI: 10.1002/dvg.23255

WILEY genesis
The Journal of Genetics and Development

RESEARCH ARTICLE

The extracellular protease *AdamTS-B* inhibits vein formation in the Drosophila wing

Minh Ngoc Pham[1] | **Mark Schuweiler**[2] | **Afshan Ismat**[2]

[1]Department of Biology, Franklin & Marshall College, Lancaster, Pennsylvania

[2]Department of Biology, University of St. Thomas, Saint Paul, Minnesota

Correspondence
Afshan Ismat, Department of Biology, University of St. Thomas, Saint Paul, MN 55105.
Email: afshan.ismat@stthomas.edu

Present address
Minh Ngoc Pham, Integrative Molecular and Biomedical Sciences/Molecular and Human Genetics, Baylor College of Medicine, Houston, TX 77030.

Funding information
University of St. Thomas

Summary

Vein patterning in the Drosophila wing provides a powerful tool to study regulation of various signaling pathways. Here we show that the ADAMTS extracellular protease *AdamTS-B* (*CG4096*) is expressed in the embryonic wing imaginal disc precursor cells and the wing imaginal disc, and functions to inhibit wing vein formation. Knock-down of *AdamTS-B* displayed posterior crossveins (PCVs) with either extra branches or deltas, or wider PCVs, and a wandering distal tip of the L5 longitudinal vein. Conversely, over-expression of *AdamTS-B* resulted in a complete absence of the PCV, an incomplete anterior crossvein, and missing distal end of the L5 longitudinal vein. We conclude that *AdamTS-B* inhibits wing vein formation through negative regulation of signaling pathways, possibly BMP as well as Egfr, displaying the complexity of roles for this family of extracellular proteases.

KEYWORDS

ADAMTS, BMP, crossvein, drosophila, wing

1 | INTRODUCTION

The extracellular matrix (ECM) surrounds all cells and tissues, and is, therefore, necessary for a majority of cellular processes, including cell migration, cell shape change, cell division, and cell–cell communication. The ECM is a dynamic structure that is constantly remodeling and restructuring itself. It houses a myriad of molecules required for the structure and physical support of cells and tissues, proteases that modify and restructure this physical support, signaling molecules that activate various signaling pathways, and extracellular modulators of these signaling pathways (O'Connor, Umulis, Othmer, & Blair, 2006; Rozario & DeSimone, 2010; Umulis, O'Connor, & Blair, 2009; Vu & Werb, 2000). With all that is known about the ECM, we still do not fully understand how interactions between cells and their external environment affect cell behavior.

The development of the Drosophila wing provides a good model to study how cells interact with their external environment because it is composed of two epithelial sheets separated by a layer of ECM (Blair, 2007; Milan, Baonza, & Garcia-Bellido, 1997; Murray, Fessler, & Palka, 1995). In this study, we examine the role of one ADAMTS extracellular protease, *CG4096* (now named *AdamTS-B*), in the formation of the veins in the wing. Our research shows that, more than just clearing out space in the ECM for morphogenetic processes, this family of proteases is an important regulator in signaling pathways necessary for cell specification.

The adult wing has a stereotypical pattern of longitudinal veins and crossveins (Figure 1a). In contrast to overall wing morphogenesis, veins are formed through specification of cell fate, not cell migration or cell shape changes (Blair, 2007; Fristrom, Wilcox, & Fristrom, 1993; Murray et al., 1995). The specification of vein territories occurs during the larval stage, and the differentiation of wing veins and intervein regions occurs during pupariation (Bangi & Wharton, 2006; Blair, 2007; de Celis, Barrio, & Kafatos, 1996; Sturtevant, Biehs, Marin, & Bier, 1997). The final veins are formed through interactions of certain signaling pathways, namely Egfr and BMP, and *AdamTS-B* could potentially interact with both of these pathways (Butchar et al., 2012; this report). Therefore, the adult wing has become a useful model to study the regulation of these signaling pathways.

There are two main signaling pathways that function in wing vein formation, Egfr and BMP (Bangi & Wharton, 2006; Blair, 2007;

Minh Ngoc Pham and Mark Schuweiler contributed equally to this study.

This work was supported by start-up funds from Franklin & Marshall College, Lancaster, PA and start-up funds from University of St. Thomas, St. Paul, MN to A.I.

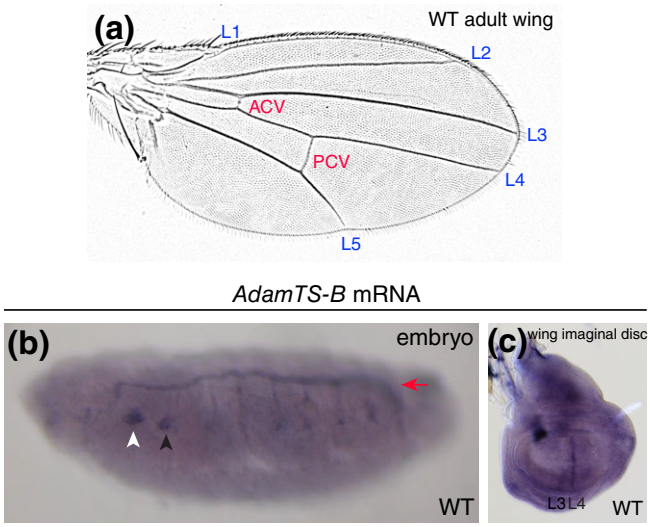

FIGURE 1 *AdamTS-B* mRNA is expressed in wing imaginal disc precursor cells and in the wing imaginal disc. (a) Wild type (WT) adult wing with longitudinal veins L1–L5 (blue), posterior cross vein (PCV), and anterior cross vein (ACV) (red) labeled. (b) Late stage WT embryo expressing *AdamTS-B* mRNA in several tracheal branches including the dorsal trunk (red arrow), and in the haltere (white arrowhead) and wing (black arrowhead) imaginal disc precursor cells. (c) Third instar wing imaginal disc expressing *AdamTS-B* mRNA in longitudinal proveins L3 and L4

Butchar et al., 2012; Conley et al., 2000; de Celis, 1997; Matsuda, Blanco, & Shimmi, 2013; Matsuda & Shimmi, 2012; Ralston & Blair, 2005; Ray & Wharton, 2001). Egfr signaling is required for the specification of wing veins starting in the third instar imaginal disc (Blair, 2007; Butchar et al., 2012; Ray & Wharton, 2001; Sturtevant, Roark, & Bier, 1993), whereas BMP signaling is required for the specification of both longitudinal provein and intervein regions in the imaginal disc, and is later required for crossvein formation during pupariation (Bangi & Wharton, 2006; Blair, 2007; Conley et al., 2000; Matsuda & Shimmi, 2012; O'Connor et al., 2006; Ralston & Blair, 2005; Sturtevant et al., 1997; Vilmos, Sousa-Neves, Lukacsovich, & Marsh, 2005).

The longitudinal veins are specified before the crossveins. The longitudinal veins start out as proveins that rely mostly on an increase in Egfr signaling within the proveins. Two of the Egf ligands, Spitz and Keren, are expressed ubiquitously throughout the wing disc, with expression increasing at later stages along the proveins (Tsruya et al., 2002; Urban, Lee, & Freeman, 2001). BMP signaling, on the other hand, is required for the maintenance of the longitudinal veins, especially the distal longitudinal veins. BMP activity in the longitudinal veins requires two ligands, Decapentaplegic (Dpp), a homolog of vertebrate BMP2/4, and Glass bottom boat (Gbb), a member of the vertebrate BMP5/6/7 subgroup (de Celis, 1997; O'Connor et al., 2006; Ray & Wharton, 2001).

BMP signaling is the primary driver for the formation of the posterior and anterior crossveins (ACVs) during pupariation (Conley et al., 2000; de Celis, 1997; Ray & Wharton, 2001). The crossveins develop much later than the longitudinal veins, from 18 to 30 hr after pupariation (Ralston & Blair, 2005). The process of crossvein formation requires transport of the Dpp-Gbb heterodimer from the adjacent longitudinal veins to the crossveins (Conley et al., 2000; Matsuda & Shimmi, 2012; Ralston & Blair, 2005; Vilmos et al., 2005). This Dpp-Gbb heterodimer is regulated extracellularly by several molecules along the way from the longitudinal veins to the posterior crossvein (PCV) region. First, the extracellular BMP-binding proteins Short gastrulation (Sog) and Crossveinless (Cv) facilitate long-range transport of the Dpp-Gbb complex from adjacent longitudinal veins to the PCV region (Ray & Wharton, 2001; Shimmi, Ralston, Blair, & O'Connor, 2005; Wang & Ferguson, 2005). Second, Tlr, a Tolloid-related protease releases the Dpp-Gbb heterodimer from the Sog-Cv complex at the PCV region (Nguyen, Jamal, Shimell, Arora, & O'Connor, 1994; O'Connor et al., 2006; Serpe, Ralston, Blair, & O'Connor, 2005; Shimmi et al., 2005; Umulis et al., 2009; Wang & Ferguson, 2005). Lastly, once at the presumptive PCV, Crossveinless-2 (Cv-2) helps Dpp-Gbb bind to BMP receptors (Conley et al., 2000; Serpe et al., 2008).

Clearly, the Egfr and BMP pathways function together to form all the veins in the wing. It is also clear that both of these pathways are heavily regulated extracellularly, to control the levels of ligand-receptor binding, and consequently, vein formation. It has been suggested that the extracellular protease *AdamTS-B* negatively regulates the Egfr pathway by sequestering the ligands Spi and Krn during formation of the L2 longitudinal vein (Butchar et al., 2012). The results of the present study indicate that *AdamTS-B* might have a role in regulating the BMP pathway as well.

In this study, we provide further characterization of the gene *AdamTS-B* in *Drosophila melanogaster*, an extracellular protease of the ADAMTS family. We demonstrate that *AdamTS-B* does function as an inhibitor of wing vein formation. Interestingly, knock-down of *AdamTS-B* using three different RNAi lines displayed PCVs with extra branches or deltas. Two of these RNAi lines also displayed an increase in extra L2 longitudinal veins, similar to results shown in Butchar et al. (2012). Conversely, over-expression of *AdamTS-B* resulted in a complete loss of the PCV, incomplete ACV, and severe shortening of the L5 longitudinal vein. These results clearly demonstrate a crucial role for *AdamTS-B* in regulating wing vein formation, including a possible role in regulating BMP signaling. These results demonstrate the complexity and interconnectedness of these two signaling pathways, Egfr and BMP, in wing-vein formation, and how one extracellular factor could possibly regulate both pathways.

2 | RESULTS

2.1 | AdamTS-B mRNA is expressed in embryonic and larval tissues

The adult wing contains five major longitudinal veins, L1–L5 (Figure 1a) and two crossveins, the ACV and the PCV (Figure 1a). These veins are formed from wide gaps between the two epithelial sheets (Bangi & Wharton, 2006; Blair, 2007; de Celis et al., 1996; Fristrom et al., 1993; Murray et al., 1995; Sturtevant et al., 1997). We know from previous work that *AdamTS-B* mRNA is expressed in the wing imaginal disc, specifically in the L3 and L4 longitudinal proveins (Butchar et al., 2012). We wanted to see whether this expression was confined to the imaginal disc, or if it extended to other stages of wing

development. *AdamTS-B* mRNA is expressed in the wing and haltere imaginal disc precursor cells in the embryo (Figure 1b, white and black arrowheads, respectively), as well as several branches of the embryonic trachea (Figure 1b, red arrow). In the wing imaginal disc, *AdamTS-B* mRNA is expressed in the L3 and L4 longitudinal proveins (Butchar et al., 2012) (Figure 1c).

2.2 | Extra L2 longitudinal veins in AdamTS-B knock-down wings is RNAi-line dependent

Based on the expression pattern of *AdamTS-B* mRNA in the wing imaginal disc precursor cells and in the imaginal disc, we wanted to examine the loss of *AdamTS-B* on wing development. A complete loss-of-function allele for *AdamTS-B* was generated through imprecise excision (A.I., unpublished), however, no adult survivors escape. Therefore, we used three different RNAi lines of *AdamTS-B* to examine the results of *AdamTS-B* knock-down for the remainder of this study. A previous study by Butchar et al. (2012) showed that knock-down of *AdamTS-B* using an RNAi line from the Vienna Drosophila Resource Center (VDRC) and a ubiquitous *Act5C*-GAL4 driver resulted in extra L2 longitudinal veins. VDRC has two RNAi lines of *AdamTS-B* (*AdamTS-B*$^{RNAi[VDRC-109025]}$ and *AdamTS-B*$^{RNAi[VDRC-108353]}$) available, and it is unclear which of these lines was used by Butchar et al. (2012). In our experiments we looked at three different RNAi lines—the two from VDRC, and one from the Transgenic RNAi Project (TRiP). First, we observed extra L2 longitudinal veins in the heterozygous *MS1096*-GAL4 control wings (Figure 2a, red arrowhead, 2G). *AdamTS-B* knock-down using the RNAi line from TRiP (*MS1096::AdamTS-B*$^{RNAi[TRiP]}$) did not display an increase in extra L2 longitudinal veins (Figure 2b,g). Second, our observations using the two RNAi lines from VDRC (*AdamTS-B*$^{RNAi[VDRC-108353]}$ and *AdamTS-B*$^{RNAi[VDRC-109025]}$), and a wing-specific GAL4 driver (*MS1096*-GAL4) (rather than ubiquitous), showed an increase in extra L2 longitudinal veins similar to those results found by Butchar et al. (2012) (Figure 2c,d, red arrowheads, 2g). Third, using a second wing-specific GAL4 driver, the heterozygous *nub*-GAL4 control wings also displayed extra L2 longitudinal veins (Figure 2e, red arrowhead, 2g) with a marked decrease in extra L2 longitudinal veins in the *AdamTS-B* knock-down wings (Figure 2f,g).

The discrepancies we observed in the L2 vein results could be due to the use of different RNAi lines of *AdamTS-B*, or possibly the different GAL4 drivers (ubiquitous versus wing-specific). We were unable to compare *AdamTS-B* knock-down with all three RNAi lines using the ubiquitous *Act5C*-GAL4 because *Act5C::AdamTS-B*$^{RNAi[TRiP]}$ was semi-lethal, with just a few adult survivors (data not shown). This conflicting data, which could be due to off-target effects in the different RNAi lines, suggests a more complicated role for *AdamTS-B* in its regulation of wing vein patterning. Overall, the results highlight the importance of this particular extracellular protease in wing vein formation and patterning.

2.3 | Knock-down of AdamTS-B displays PCV with an extra branch or delta

Normally, the PCV forms as a straight line between the L4 and L5 longitudinal veins (Figures 1a, 3a). In contrast, knock-down of *AdamTS-B*

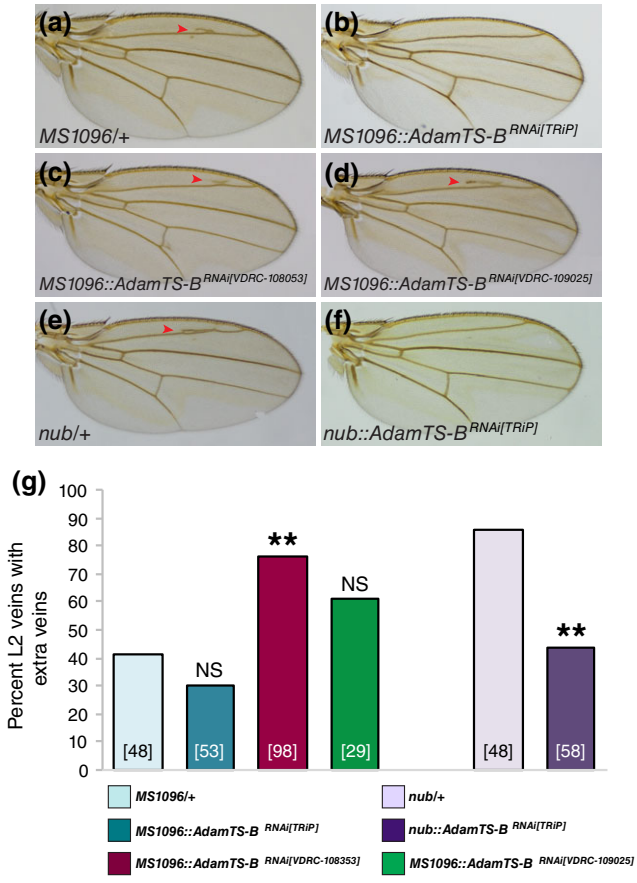

FIGURE 2 Extra L2 veins in *AdamTS-B* knock-down wings is RNAi-line dependent. (a) Control wing (*MS1096/+*) displaying extra L2 vein (red arrowhead). (b) *AdamTS-B* knock-down wing (*MS1096::AdamTS-B*$^{RNAi[TRiP]}$) does not display extra L2 veins. (c) *AdamTS-B* knock-down wing (*MS1096::AdamTS-B*$^{RNAi[VDRC-108353]}$) displaying extra L2 veins (red arrowhead). (d) *AdamTS-B* knock-down wing (*MS1096::AdamTS-B*$^{RNAi[VDRC-109025]}$) displaying extra L2 veins (red arrowhead). (e) Control wing (*nub/+*) displaying extra L2 vein (red arrowhead). Quantification of percentage of total wings displaying defects in L5 vein. (f) *AdamTS-B* knock-down wing (*nub::AdamTS-B*$^{RNAi[TRiP]}$) does not display extra L2 veins. (g) Quantification of percent L2 veins with extra veins. Only the knock-down of *AdamTS-B* using the Vienna Drosophila Resource Center (VDRC) RNAi lines (maroon and green bars) displayed an increase in extra L2 veins compared to control (light blue bar). Number of wings scored for each genotype is shown in brackets in each bar. $^{**}p < .05$ based on a G-test of statistical independence

with all three RNAi lines (*MS1096::AdamTS-B*$^{RNAi[TRiP]}$, *MS1096::AdamTS-B*$^{RNAi[VDRC-108353]}$, and *MS1096::AdamTS-B*$^{RNAi[VDRC-109025]}$) displayed either an extra branch on the PCV or a delta at the PCV (Figure 3b–d, red arrowheads). When quantified, there was a 20% increase in the percent of *AdamTS-B*$^{RNAi[TRiP]}$ wings that displayed PCVs with an extra branch or delta compared to the control (Figure 3e). *AdamTS-B* knock-down using the two VDRC RNAi lines (*VDRC-109025* and *VDRC-108353*) displayed an even higher increase in PCVs with an extra branch or delta, 40% and 50%, respectively (Figure 3e).

In addition to the extra branch or delta at the PCVs seen in the *AdamTS-B* knock-down, we also observed that in wings that did not display extra PCVs, the PCV was wider than control PCVs. To quantify

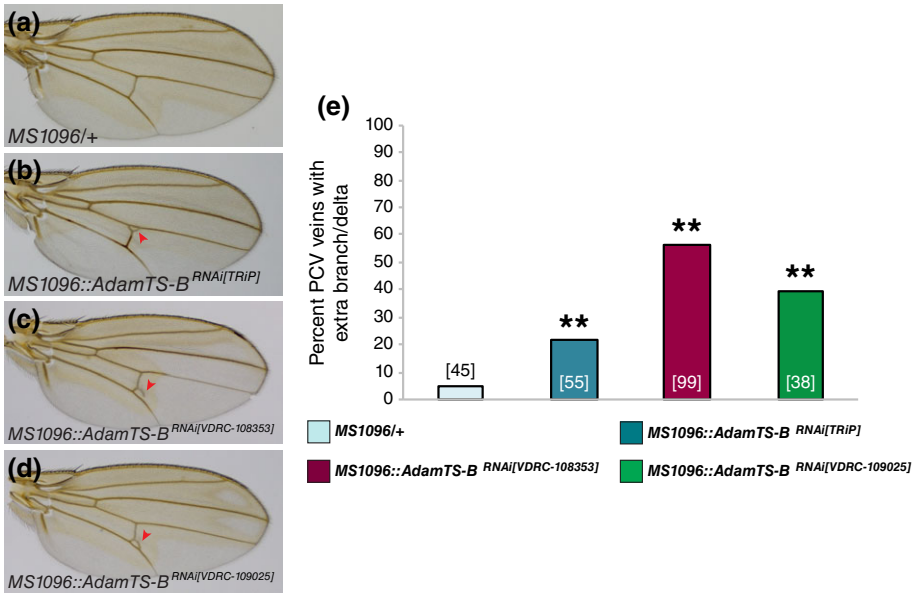

FIGURE 3 Knock-down of *AdamTS-B* displays posterior cross vein (PCV) veins with an extra branch or delta. All wings are from crosses using *MS1096*-GAL4. (a) Control wing (*MS1096/+*) displaying a straight PCV. (b) *AdamTS-B* knock-down wing (*MS1096::AdamTS-B*$^{RNAi[TRiP]}$) displaying a delta at the anterior end of the PCV (red arrowhead). (c) *AdamTS-B* knock-down wing (*MS1096::AdamTS-B*$^{RNAi[VDRC\text{-}108353]}$) displaying an extra branch at the posterior end of the PCV (red arrowhead). (d) *AdamTS-B* knock-down wing (*MS1096::AdamTS-B*$^{RNAi[VDRC\text{-}109025]}$) displaying a delta at the posterior end of the PCV (red arrowhead). (e) Quantification of the percent PCV veins with an extra branch or delta. All three RNAi lines of AdamTS-B displayed an increase in extra branch or deltas at the PCV. Number of wings scored for each genotype is shown in brackets in each bar. $^{**}p < .05$ based on a G-test of statistical independence

this we measured the width of the PCV veins at three positions (Top, Middle, and Bottom) in both heterozygous control wings of three GAL4 lines (*MS1096/+*, *nub/+*, and *en/+*) (Figure 4a′,c′,e′,g) and *AdamTS-B*$^{RNAi[TRiP]}$ (Figure 4b′,d′,f′,g). *AdamTS-B*$^{RNAi[TRiP]}$ wings that did not display an extra branch or delta at the PCV were significantly wider at the top, middle, and bottom, as compared to control wings (Figure 4b′,d′,f′,g′). As already suggested by the incongruities in extra L2 veins (Figures 2, Supporting Information S1), these results also suggest a complicated role for *AdamTS-B* as a negative extracellular regulator of wing vein formation, due to the possibility that variations in the level of knock-down of this one gene could manifest itself in different PCV defects.

2.4 | Knock-down of AdamTS-B displays wandering L5 longitudinal veins

In control wings of three GAL4 lines (*MS1096/+*, *nub/+*, and *en/+*), the L5 longitudinal vein reaches the posterior margin and tapers at the end (Figures 1a, 5a′,c′,e′). Knock-down of *AdamTS-B* (*AdamTS-B*$^{RNAi[TRiP]}$) using these three GAL4 lines displayed wandering L5 longitudinal vein (Figure 5b′,d′,f′, red arrowheads). When we quantified this, more than 40% of *AdamTS-B*$^{RNAi[TRiP]}$ wings had wandering L5 veins compared to control wings (Figure 5g).

2.5 | Over-expression of AdamTS-B displays complete loss of PCV and loss of distal L5 longitudinal vein

Since the knock-down of *AdamTS-B* displayed an extra branch or delta at the PCV and wandering L5 longitudinal veins, we were curious about what phenotype(s) the over-expression of *AdamTS-B* might display. Over-expression of *AdamTS-B* resulted in dramatic defects in both crossveins and L5 longitudinal veins using three different GAL4 lines (*MS1096*-GAL4, *nub*-GAL4, and *en*-GAL4). First, 100% of *AdamTS-B* over-expression wings displayed a missing distal portion of the L5 longitudinal vein (Figure 6b,d,f,g). Second, almost 100% of *AdamTS-B* over-expression wings displayed a completely missing PCV (Figure 6b,d,f, between red asterisks, and 6g). Third, almost 100% of *AdamTS-B* over-expression wings displayed an incomplete ACV (Figure 6b,d,f, yellow arrowhead, and 6g). Clearly, the over-expression of *AdamTS-B* displaying a complete loss of PCV, an incomplete ACV, and missing distal L5 longitudinal vein illustrates an antagonistic role for *AdamTS-B* in vein formation.

2.6 | Loss or gain of AdamTS-B changes overall wing shape

In addition to our observations that the *AdamTS-B* over-expression wings were completely missing the PCV, and had a much shorter L5 longitudinal vein, we also noticed that the overall shape of these wings was different from control wings. We decided to measure the overall length and width of *AdamTS-B* over-expression wings compared to control, as well as *AdamTS-B*$^{RNAi[TRiP]}$ knock-down wings compared to control wings. The length of the wing was measured from the L2–L3 intersection to the distal end of L3 (length, measured in mm) (Figure 7a, yellow line). The width was measured as the length of the line perpendicular to the length line, intersecting that line at its midpoint (width, measured in mm) (Figure 7a, purple line). The overall shape of the *AdamTS-B* over-expression wing was longer with a pointier distal end (end of the L3 longitudinal vein, Figure 7c compared to

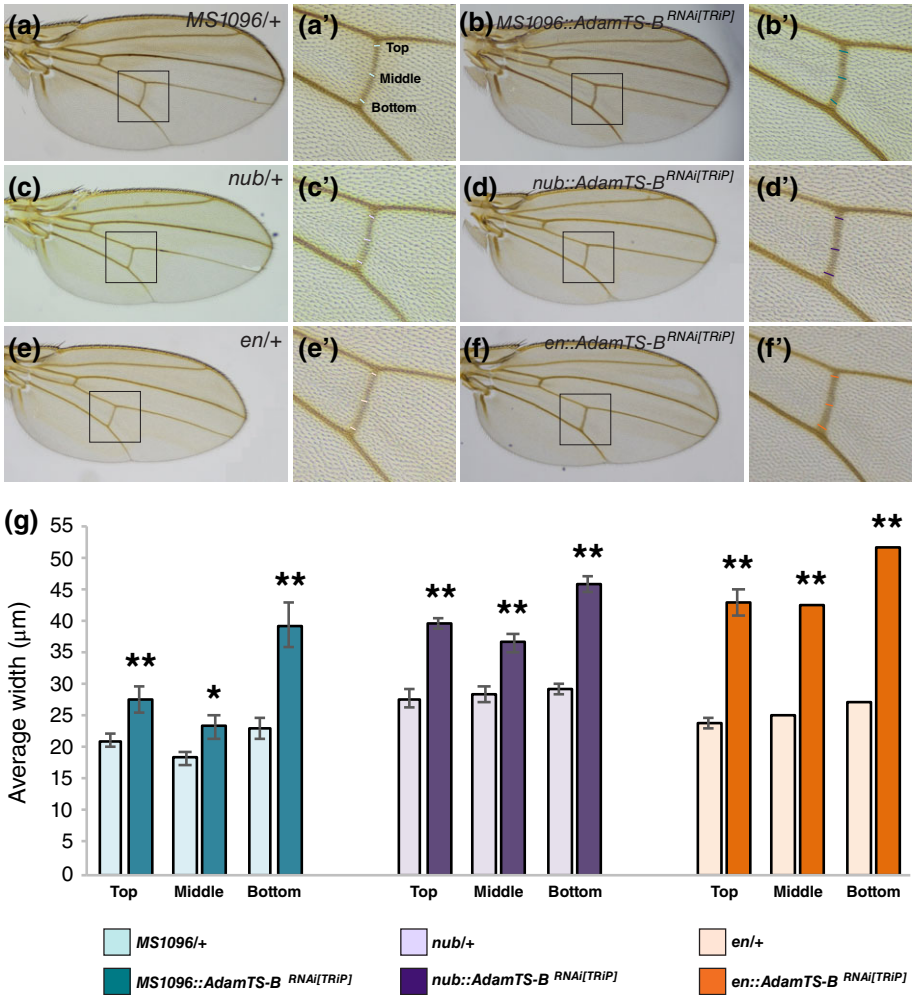

FIGURE 4 Knock-down of *AdamTS-B* results in wider PCV vein. The width of the PCV vein was measured at three points along the vein (top, middle, and bottom). (a) Control wing (*MS1096/+*). (a′) Enlargement of boxed region in (a). Top, middle, and bottom widths represented by light blue lines. (b) *AdamTS-B* knock-down wing (*MS1096::AdamTS-B*$^{RNAi[TRiP]}$). (b′) Enlargement of boxed region in (b). Top, middle, and bottom widths represented by dark turquoise lines. (c) Control wing (*nub/+*). (c′) Enlargement of boxed region in (c). Top, middle, and bottom widths represented by light purple lines. (d) *AdamTS-B* knock-down wing (*nub::AdamTS-B*$^{RNAi[TRiP]}$). (d′) Enlargement of boxed region in (d). Top, middle, and bottom widths represented by dark purple lines. (e) Control wing (*en/+*). (e′) Enlargement of boxed region in (e). Top, middle, and bottom widths represented by light orange lines. (f) *AdamTS-B* knock-down wing (*en::AdamTS-B*$^{RNAi[TRiP]}$). (f′) Enlargement of boxed region in (f). Top, middle, and bottom widths represented by dark orange lines. (g) Quantification of average measurements for controls (*MS1096/+*) (light blue bars), (*nub/+*) (light purple bars) and (*en/+*) (light orange bars), and knock-down of *AdamTS-B* (*AdamTS-B*$^{RNAi[TRiP]}$) (dark turquoise, dark purple, and dark orange bars) of top widths, middle widths, and bottom widths. Number of measurements taken for each genotype: *MS1096/+* and *MS1096::AdamTS-B*$^{RNAi[TRiP]}$ [n = 16], *nub/+* and *nub::AdamTS-B*$^{RNAi[TRiP]}$ [n = 20], *en/+* and *en::AdamTS-B*$^{RNAi[TRiP]}$ [n = 17]. Data are expressed as width in µm ± *SEM*. Statistical significance was determined at *p < .05 using Students two-tailed t test and **p < .001 using Students two-tailed t test

7a,b) and a shorter width. Indeed, comparing the mean length/width ratios, the over-expression of *AdamTS-B* had a ratio of approximately 1.9, compared to a ratio of approximately 1.7 for the control (Figure 7d). Surprisingly, loss of *AdamTS-B* also displayed a slightly larger length/width ratio than the control (Figure 7d). The same ratios were observed using *en*-GAL4 (data not shown). From this data, we conclude that changes in the PCV, whether it is missing or there are extra branches, affect the overall shape of the wing.

3 | DISCUSSION

Taken together, our findings provide more evidence that the extracellular protease *AdamTS-B* functions as an inhibitor of wing vein formation. Specifically, we demonstrated that knock-down of *AdamTS-B* resulted in an extra branch or delta at the PCV (Figure 3), as well as defects in distal portions of the L5 longitudinal veins (Figure 5). Depending on the RNAi line used to knock-down *AdamTS-B*, we did or did not observe an increase in extra L2 longitudinal veins (Figure 2). Additionally, over-expression of *AdamTS-B* resulted in a complete loss of the PCV and distal L5 longitudinal veins, as well as an incomplete ACV (Figure 6). As Butchar et al. (2012) showed previously, ADAMTS proteases not only function to degrade components of the ECM, but can also function to promote or prevent ligand-receptor binding. Our results help to confirm a role for *AdamTS-B* in negatively regulating wing vein formation, but the conflicting knock-down results between Butchar et al. (2012) and this report also underscore the complexity of this process.

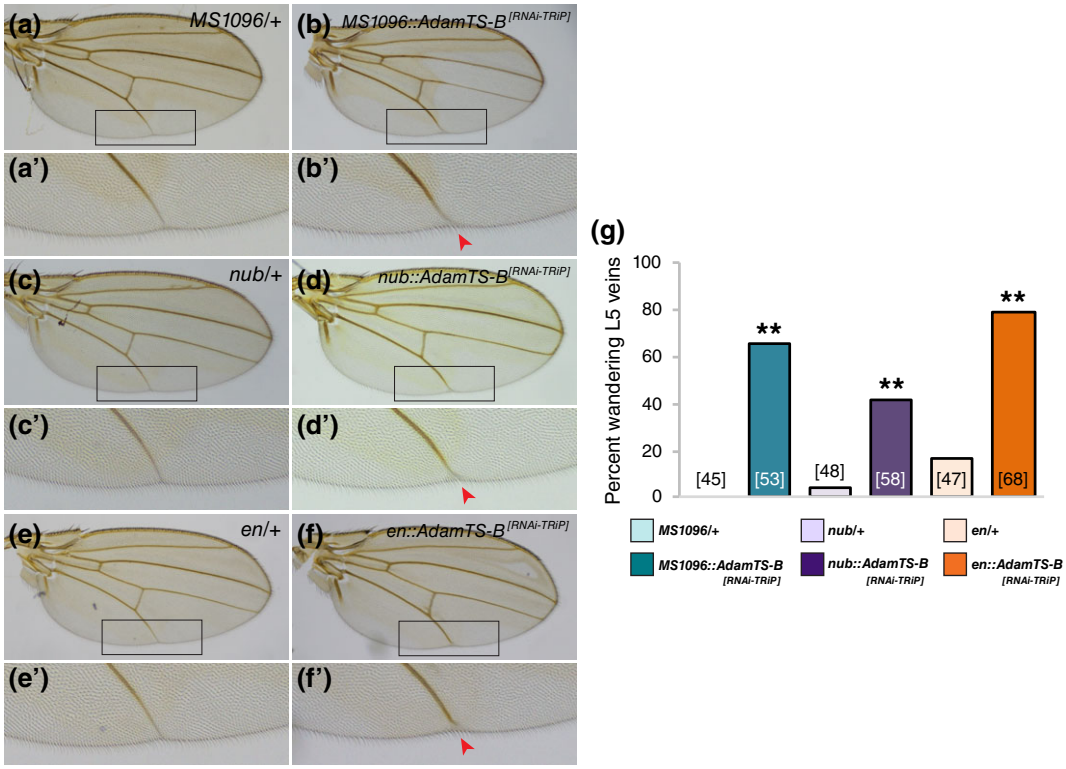

FIGURE 5 Knock-down of *AdamTS-B* displays wandering L5 veins. (a) Control wing (*MS1096/+*). (a′) Enlargement of boxed region in (a) showing the L5 vein tapering and fully reaching the posterior edge of the wing. (b) *AdamTS-B* knock-down wing (*MS1096::AdamTS-B*$^{RNAi[TRiP]}$). (b′) Enlargement of boxed region in (b) showing a wandering L5 vein (red arrowhead). (c) Control wing (*nub/+*). (c′) Enlargement of boxed region in (c) showing tapered L5 vein. (d) *AdamTS-B* knock-down wing (*nub::AdamTS-B*$^{RNAi[TRiP]}$). (d′) Enlargement of boxed region in (d) showing a wandering L5 vein (red arrowhead). (e) Control wing (*en/+*). (e′) Enlargement of boxed region in (c) showing tapered L5 vein. (d) *AdamTS-B* knock-down wing (*en::AdamTS-B*$^{RNAi[TRiP]}$). (d′) Enlargement of boxed region in (d) showing a wandering L5 vein (red arrowhead). (g) Quantification of percent wandering L5 veins. Number of wings scored for each genotype is shown in brackets in each bar. $^{**}p < .05$ based on a G-test of statistical independence

3.1 | AdamTS-B as a negative regulator of Egfr and BMP signaling in wing vein formation?

Previous literature on the other two Drosophila ADAMTSs (*AdamTS-A* and *stl*), as well as previous reports on mammalian ADAMTSs, have indicated that the main function of these particular extracellular proteases is to restructure the ECM for morphogenetic processes (Blelloch et al., 1999; Cal, Arguelles, Fernandez, & Lopez-Otin, 2001; Enomoto et al., 2010; Ismat, Cheshire, & Andrew, 2013; Lhamo & Ismat, 2015; Liu, 2009; McCulloch et al., 2009; Nakada et al., 2005; Nishiwaki, Hisamoto, & Matsumoto, 2000; Surridge et al., 2009; Wagstaff, Kelwick, Decock, & Edwards, 2011; Wei, Richbourgh, Jia, & Liu, 2014; Xie et al., 2016). Vein formation in the wing is due to cell fate, and not cell migration or cell shape changes (Blair, 2007; Fristrom et al., 1993; Murray et al., 1995). The fate of cells induced to become a vein cell versus an intervein cell is the result of signaling pathways, including Egfr and BMP (Bangi & Wharton, 2006; Blair, 2007; de Celis et al., 1996; Sturtevant et al., 1997).

We show here that *AdamTS-B* functions to prevent wing vein formation. Does *AdamTS-B* work through the Egfr pathway or the BMP pathway, or both? *AdamTS-B* mRNA expression is upregulated when Egfr signaling is activated, however, not to the extent that would be expected if Egfr activity was the only factor that affected *AdamTS-B* expression (Butchar et al., 2012). The next question to answer would be whether *AdamTS-B* is a target of BMP signaling. Butchar et al. (2012) demonstrated a role for *AdamTS-B* in negatively regulating the Egfr pathway during wing vein formation (as seen by extra L2 longitudinal veins), whereas we bring up the possibility that this same extracellular protease, *AdamTS-B*, could also function through the BMP pathway to inhibit vein formation (associated with the PCV and ACV). Using two RNAi lines from VDRC, the same resource used by Butchar et al., and a wing-specific GAL4 driver, we observed the same increase in extra L2 longitudinal veins (Figure 2). However, the RNAi line from a different resource, TRiP, did not show an increase in extra L2 longitudinal veins (Figure 2). It is clear that these three RNAi lines differ, and there may be off-target effects with the VDRC RNAi lines that could affect defects observed in the *AdamTS-B* knock-down.

Regulation of signaling pathways is complex and muddled. The close interweaving of Egfr and BMP signaling in wing vein patterning makes it difficult to parse out the exact role of each pathway in the patterning of each vein. The adult wing phenotypes seen in both the knock-down and over-expression of *AdamTS-B* point toward a role for this extracellular protease in regulating BMP activity, as the phenotypes seen in the PCV and ACV resemble that seen in other regulators of BMP activity, like Gbb and Cv-2 (Bangi & Wharton, 2006; Conley et al., 2000). First, knock-down of *AdamTS-B* using the three different RNAi lines displayed PCVs with extra branches or deltas (Figure 3). But the situation must be more complicated than that, because the VDRC knock-downs showed a much higher percentage of PCVs with extra branches or deltas than the TRiP line, but a much lower

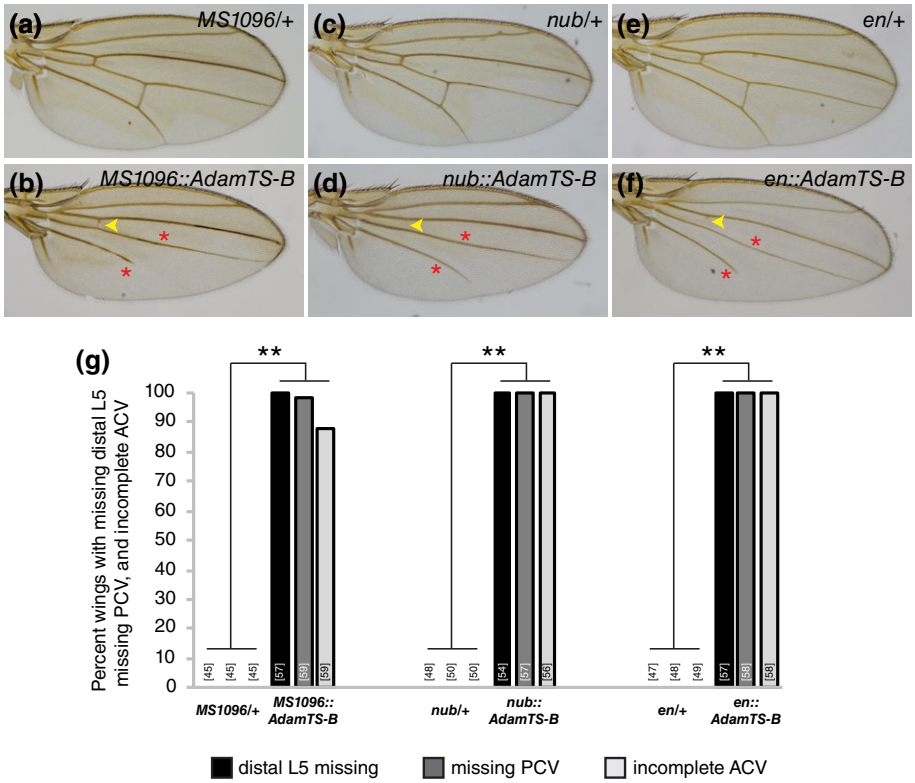

FIGURE 6 Over-expression of *AdamTS-B* displays complete absence of PCV, missing distal L5 vein, and incomplete ACV. (a) Control wing (*MS1096/+*) displaying a single PCV between L4 and L5 veins, and full length L5 vein reaching the posterior edge of the wing, and complete ACV between L3 and L4 veins. (b) Over-expression of *AdamTS-B* (*MS1096::AdamTS-B*) displays a complete absence of the PCV (between red asterisks), missing distal L5 vein, and an incomplete ACV (yellow arrowhead). (c) Control wing (*nub/+*). (d) Over-expression of *AdamTS-B* (*nub::AdamTS-B*) displays a complete absence of the PCV (between red asterisks), missing distal L5 vein, and complete absence of ACV (yellow arrowhead). (e) Control wing (*en/+*). (f) Over-expression of *AdamTS-B* (*en::AdamTS-B*) displays a complete absence of the PCV (between red asterisks), missing distal L5 vein, and complete absence of ACV (yellow arrowhead). (g) Quantification of percent wings displaying missing distal L5 vein, completely missing PCV, and incomplete ACV. Almost identical defects were seen over-expressing *AdamTS-B* using three different GAL4 lines. Number of wings scored for each genotype is shown in brackets in each bar. $^{**}p < .05$ based on a G-test of statistical independence for each defect compared to the control

percentage of L5 longitudinal vein defects than the TRiP line (Figures 3 and 5 and data not shown), and the TRiP knock-down did not show an increase in extra L2 longitudinal veins (Figure 2). These results demonstrate that any interaction of *AdamTS-B* with Egfr and BMP pathways in vein formation is a complex combination of factors—the location of this protein in the wing (the L2 longitudinal vein is far from the PCV), the timing (the longitudinal veins are specified much earlier than the crossveins), and the level of AdamTS-B protein. Previous research has shown that these two pathways work together from the third instar stage to form the longitudinal and crossveins (Blair, 2007; de Celis, 1997), so this interweaving of Egfr and BMP pathway regulation that our results suggest is consistent with those findings.

Second, over-expressing *AdamTS-B* throughout the wing results in a complete loss of the PCV, severe shortening of the L5 longitudinal vein, and incomplete ACV (Figure 6). The absence of the PCV or ACV and distal portion of the L5 longitudinal vein is seen when BMP activity is inhibited, especially when either of the ligands Dpp or Gbb are absent (de Celis, 1997; Ray & Wharton, 2001). Formation of the crossveins, as well as maintenance of the distal longitudinal veins, relies on proper levels of BMP signaling (Conley et al., 2000; Ralston & Blair, 2005; Ray & Wharton, 2001). Butchar et al. (2012) demonstrated genetic interactions between *AdamTS-B* and Egfr ligands *spi* and *krn* or *krn* and *vn*. Our over-expression data further emphasizes the possibility that this extracellular protease has a more complicated role, perhaps in regulating BMP signaling as well as Egfr signaling. Further molecular work examining BMP activity levels will help to verify whether *AdamTS-B* actually regulates BMP signaling directly.

4 | METHODS

4.1 | Drosophila strains

The following Drosophila strains were used in this study: Canton S (CS), *MS1096*-GAL4, *UAS-dcr2; nubbin*-GAL4, *en*-GAL4, *Act5C*-GAL4 (Bloomington Drosophila Stock Center, Indiana University, Bloomington, IN), *UAS-AdamTS-B*$^{RNAi[TRiP]}$ (TRiP number HMC02914) (DRSC/TRiP Functional Genomics Resources, Harvard University, Cambridge, MA), *UAS-AdamTS-B*$^{RNAi[VDRC\text{-}109025]}$ and *UAS-AdamTS-B*$^{RNAi[VDRC\text{-}108053]}$ (VDRC numbers 108353 and 109025).

4.2 | Construction of UAS-AdamTS-B and UAS-AdamTS-B-GFP

UAS-AdamTS-B and the C-terminal tagged *UAS-AdamTS-B-GFP* were generated by sub-cloning the full length cDNA of *AdamTS-B*

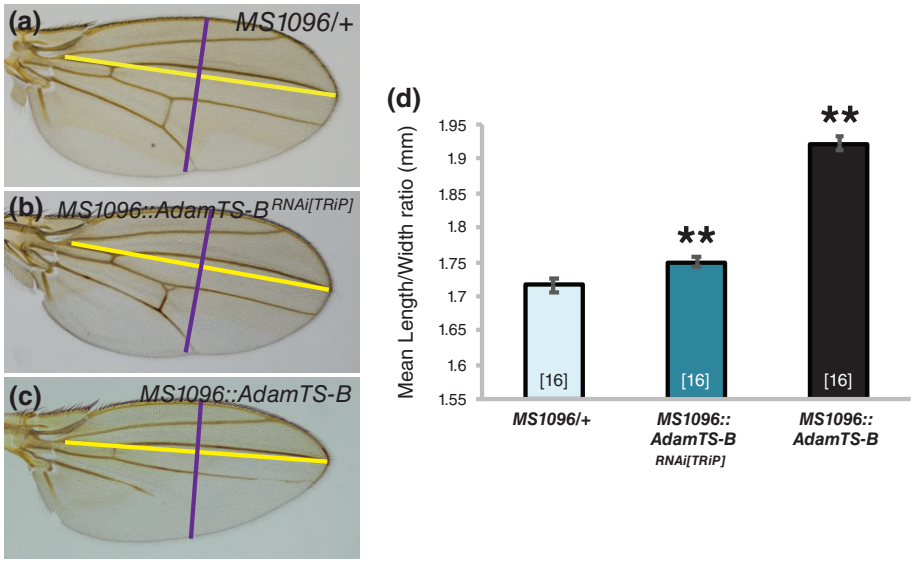

FIGURE 7 Loss or gain of *AdamTS-B* change in overall wing size and shape. The length of each wing was measured from the intersection of the L2 and L3 veins to the distal tip of the L3 vein (yellow line in a–c). The width of each wing was measured perpendicular from a point equidistant on the length (purple line in a–c). (a–c) Example wings from control (*MS1096/+*), loss of *AdamTS-B* (*MS1096::AdamTS-B*$^{RNAi[TRiP]}$), and *AdamTS-B* over-expression (*MS1096::AdamTS-B*) showing length and width lines. (d) Mean length/width ratios for control (white bar), loss of *AdamTS-B* (black bar), over-expression of untagged *AdamTS-B* (light gray bar), and GFP-tagged *AdamTS-B* (dark gray bar). Number of measurements taken for each genotype is shown in brackets in each bar. Data are expressed as length/width ratio ± *SEM*. Statistical significance was determined at $^{**}p < .05$ using Students two-tailed *t* test

(GH22104) into the Gateway vectors (http://emb.carnegiescience.edu/labs/murphy/Gateway%20vectors.html) through LR recombinase (Invitrogen). Reagents available upon request.

4.3 | Genetics

Adult wing samples: Females of Canton S (CS), *UAS-AdamTS-B*$^{RNAi[TRiP]}$ (TRiP), *UAS-AdamTS-B*$^{RNAi[VDRC\text{-}109025]}$, and *UAS-AdamTS-B*$^{RNAi[VDRC\text{-}108353]}$, *UAS-AdamTS-B* crossed to males of the following GAL4 lines: *MS1096*-GAL4, *nubbin*-GAL4 (*nub*-GAL4), *en*-GAL4, and *Act5C*-GAL4. Only wings from female progeny were used for further analysis. All crosses were kept at 25 °C.

4.4 | Staining procedures

In situ hybridization of embryos and third instar wing imaginal discs were performed as described previously (Azpiazu & Frasch, 1993; Classen, Aigouy, Giangrande, & Eaton, 2008; Knirr, Azpiazu, & Frasch, 1999; Ralston & Blair, 2005; Reuter & Scott, 1990). The following digoxigenin-labeled RNA was used: *AdamTS-B* cDNA (GH22104).

4.5 | Adult wing sample preparation

Adult wings were dehydrated in 100% ethanol for 3 s and mounted in Gray's mounting media (1:4 Canada balsam:methyl salicylate).

4.6 | Wing defect analysis

Defects in wing veins were recorded, and the occurrence frequency for each defect in all genotypes was determined. The wing vein defects were recorded as either absent or present. The defect occurrence frequencies were compared among Drosophila strains using a G-test of independence.

4.7 | Imaging

Imaginal discs and adult wings were imaged using brightfield optics on a Nikon Eclipse CiL compound light microscope at 4× and 10× magnifications. Embryos were imaged using differential interference contrast optics on a Nikon Eclipse CiL compound light microscope at 20× magnification.

4.8 | Adult wing length/width measurements

A ratio of the length (from intersection of L2 and L3 to the end of L3) and width (perpendicular line equidistant of the length) of 16 adult wings each from the following genotypes: *MS1096*-GAL4/+, *MS1096*-GAL4::*UAS-AsamTS-B*$^{RNAi[TRiP]}$, and *MS1096*-GAL4::*UAS-AdamTS-B* were taken of adult wings using ImageJ software and converted from pixels to mm.

4.9 | Adult wing PCV width measurements

The width at three positions along the PCV vein (Top, Middle, and Bottom) was measured from control (*MS1096*-GAL4/+), (*nub*-GAL4/+), and (*en*-GAL4/+) adult wings and *AdamTS-B* knock-down (*MS1096*-GAL4;*UAS-AsamTS-B*$^{RNAi[TRiP]}$), (*nub*-GAL4;*UAS-AsamTS-B*$^{RNAi[TRiP]}$), and (*en*-GAL4;*UAS-AsamTS-B*$^{RNAi[TRiP]}$) adult wings using ImageJ software and converted from pixels to micrometer.

ACKNOWLEDGMENTS

The authors would like to thank Gregory Berry for his encouragement and intellectual discussions, critical reading, insight, and copyediting of

the manuscript, and A. Verhoeven and K. Carlson for their comments on the manuscript. M.P. and M.S. performed all the experiments and conducted all the statistical analyses. M.P., M.S, and A.I. wrote the article.

ORCID

Afshan Ismat http://orcid.org/0000-0002-3052-3414

REFERENCES

Azpiazu, N., & Frasch, M. (1993). *tinman* and *bagpipe*: Two homeo box genes that determine cell fates in the dorsal mesoderm of *Drosophila*. *Genes & Development*, *7*, 1325–1340.

Bangi, E., & Wharton, K. (2006). Dpp and gbb exhibit different effective ranges in the establishment of the BMP activity gradient critical for *Drosophila* wing patterning. *Developmental Biology*, *295*(1), 178–193.

Blair, S. S. (2007). Wing vein patterning in *Drosophila* and the analysis of intercellular signaling. *Annual Review of Cell and Developmental Biology*, *23*, 293–319.

Blelloch, R., Anna-Arriola, S. S., Gao, D., Li, Y., Hodgkin, J., & Kimble, J. (1999). The gon-1 gene is required for gonadal morphogenesis in *Caenorhabditis elegans*. *Developmental Biology*, *216*(1), 382–393.

Butchar, J. P., Cain, D., Manivannan, S. N., McCue, A. D., Bonanno, L., Halula, S., … Simcox, A. (2012). New negative feedback regulators of Egfr signaling in *Drosophila*. *Genetics*, *191*(4), 1213–1226.

Cal, S., Arguelles, J. M., Fernandez, P. L., & Lopez-Otin, C. (2001). Identification, characterization, and intracellular processing of ADAM-TS12, a novel human disintegrin with a complex structural organization involving multiple thrombospondin-1 repeats. *The Journal of Biological Chemistry*, *276*(21), 17932–17940.

Classen, A. K., Aigouy, B., Giangrande, A., & Eaton, S. (2008). Imaging drosophila pupal wing morphogenesis. *Methods in Molecular Biology*, *420*, 265–275.

Conley, C. A., Silburn, R., Singer, M. A., Ralston, A., Rohwer-Nutter, D., Olson, D. J., … Blair, S. S. (2000). Crossveinless 2 contains cysteine-rich domains and is required for high levels of BMP-like activity during the formation of the cross veins in *Drosophila*. *Development*, *127*(18), 3947–3959.

de Celis, J. F. (1997). Expression and function of decapentaplegic and thick veins during the differentiation of the veins in the *Drosophila* wing. *Development*, *124*(5), 1007–1018.

de Celis, J. F., Barrio, R., & Kafatos, F. C. (1996). A gene complex acting downstream of dpp in *Drosophila* wing morphogenesis. *Nature*, *381*(6581), 421–424.

Enomoto, H., Nelson, C. M., Somerville, R. P., Mielke, K., Dixon, L. J., Powell, K., & Apte, S. S. (2010). Cooperation of two ADAMTS metalloproteases in closure of the mouse palate identifies a requirement for versican proteolysis in regulating palatal mesenchyme proliferation. *Development*, *137*(23), 4029–4038.

Fristrom, D., Wilcox, M., & Fristrom, J. (1993). The distribution of PS integrins, laminin a and F-actin during key stages in *Drosophila* wing development. *Development*, *117*(2), 509–523.

Ismat, A., Cheshire, A. M., & Andrew, D. J. (2013). The secreted *AdamTS-A* metalloprotease is required for collective cell migration. *Development*, *140*(9), 1981–1993.

Knirr, S., Azpiazu, N., & Frasch, M. (1999). The role of the NK homeobox gene *slouch (S59)* in somatic muscle patterning. *Development*, *126*, 4525–4535.

Lhamo, T., & Ismat, A. (2015). The extracellular protease *stl* functions to inhibit migration of v'ch1 sensory neuron during *Drosophila* embryogenesis. *Mechanisms of Development*, *137*, 1–10.

Liu, C. J. (2009). The role of ADAMTS-7 and ADAMTS-12 in the pathogenesis of arthritis. *Nature Clinical Practice Rheumatology*, *5*(1), 38–45.

Matsuda, S., Blanco, J., & Shimmi, O. (2013). A feed-forward loop coupling extracellular BMP transport and morphogenesis in *Drosophila* wing. *PLoS Genetics*, *9*(3), e1003403.

Matsuda, S., & Shimmi, O. (2012). Directional transport and active retention of dpp/BMP create wing vein patterns in drosophila. *Developmental Biology*, *366*(2), 153–162.

McCulloch, D. R., Nelson, C. M., Dixon, L. J., Silver, D. L., Wylie, J. D., Lindner, V., … Apte, S. S. (2009). ADAMTS metalloproteases generate active versican fragments that regulate interdigital web regression. *Developmental Cell*, *17*(5), 687–698.

Milan, M., Baonza, A., & Garcia-Bellido, A. (1997). Wing surface interactions in venation patterning in *Drosophila*. *Mechanisms of Development*, *67*(2), 203–213.

Murray, M. A., Fessler, L. I., & Palka, J. (1995). Changing distributions of extracellular matrix components during early wing morphogenesis in *Drosophila*. *Developmental Biology*, *168*(1), 150–165.

Nakada, M., Miyamori, H., Kita, D., Takahashi, T., Yamashita, J., Sato, H., … Okada, Y. (2005). Human glioblastomas overexpress ADAMTS-5 that degrades brevican. *Acta Neuropathologica*, *110*(3), 239–246.

Nguyen, T., Jamal, J., Shimell, M. J., Arora, K., & O'Connor, M. B. (1994). Characterization of tolloid-related-1: A BMP-1-like product that is required during larval and pupal stages of *Drosophila* development. *Developmental Biology*, *166*(2), 569–586.

Nishiwaki, K., Hisamoto, N., & Matsumoto, K. (2000). A metalloprotease disintegrin that controls cell migration in *Caenorhabditis elegans*. *Science*, *288*(5474), 2205–2208.

O'Connor, M. B., Umulis, D., Othmer, H. G., & Blair, S. S. (2006). Shaping BMP morphogen gradients in the *Drosophila* embryo and pupal wing. *Development*, *133*(2), 183–193.

Ralston, A., & Blair, S. S. (2005). Long-range dpp signaling is regulated to restrict BMP signaling to a crossvein competent zone. *Developmental Biology*, *280*(1), 187–200.

Ray, R. P., & Wharton, K. A. (2001). Context-dependent relationships between the BMPs gbb and dpp during development of the *Drosophila* wing imaginal disk. *Development*, *128*(20), 3913–3925.

Reuter, R., & Scott, M. P. (1990). Expression and function of the homeotic genes *Antennapedia* and *Sex combs reduced* in the embryonic midgut of *Drosophila*. *Development*, *109*, 289–303.

Rozario, T., & DeSimone, D. W. (2010). The extracellular matrix in development and morphogenesis: A dynamic view. *Developmental Biology*, *341*(1), 126–140.

Serpe, M., Ralston, A., Blair, S. S., & O'Connor, M. B. (2005). Matching catalytic activity to developmental function: Tolloid-related processes sog in order to help specify the posterior crossvein in the *Drosophila* wing. *Development*, *132*(11), 2645–2656.

Serpe, M., Umulis, D., Ralston, A., Chen, J., Olson, D. J., Avanesov, A., … Blair, S. S. (2008). The BMP-binding protein crossveinless 2 is a short-range, concentration-dependent, biphasic modulator of BMP signaling in *Drosophila*. *Developmental Cell*, *14*(6), 940–953.

Shimmi, O., Ralston, A., Blair, S. S., & O'Connor, M. B. (2005). The crossveinless gene encodes a new member of the twisted gastrulation family of BMP-binding proteins which, with short gastrulation, promotes BMP signaling in the crossveins of the *Drosophila* wing. *Developmental Biology*, *282*(1), 70–83.

Sturtevant, M. A., Biehs, B., Marin, E., & Bier, E. (1997). The Spalt gene links the A/P compartment boundary to a linear adult structure in the *Drosophila* wing. *Development*, *124*(1), 21–32.

Sturtevant, M. A., Roark, M., & Bier, E. (1993). The *Drosophila* rhomboid gene mediates the localized formation of wing veins and interacts genetically with components of the EGF-R signaling pathway. *Genes and Development*, *7*(6), 961–973.

Surridge, A. K., Rodgers, U. R., Swingler, T. E., Davidson, R. K., Kevorkian, L., Norton, R., … Clark, I. M. (2009). Characterization and regulation of ADAMTS-16. *Matrix Biology*, *28*(7), 416–424.

Tsruya, R., Schlesinger, A., Reich, A., Gabay, L., Sapir, A., & Shilo, B. Z. (2002). Intracellular trafficking by star regulates cleavage of the *Drosophila* EGF receptor ligand spitz. *Genes and Development*, *16*(2), 222–234.

Umulis, D., O'Connor, M. B., & Blair, S. S. (2009). The extracellular regulation of bone morphogenetic protein signaling. *Development*, *136*(22), 3715–3728.

Urban, S., Lee, J. R., & Freeman, M. (2001). *Drosophila* rhomboid-1 defines a family of putative intramembrane serine proteases. *Cell*, *107*(2), 173–182.

Vilmos, P., Sousa-Neves, R., Lukacsovich, T., & Marsh, J. L. (2005). Crossveinless defines a new family of twisted-gastrulation-like modulators

of bone morphogenetic protein signalling. *EMBO Reports*, *6*(3), 262–267.

Vu, T. H., & Werb, Z. (2000). Matrix metalloproteinases: Effectors of development and normal physiology. *Genes and Development*, *14*(17), 2123–2133.

Wagstaff, L., Kelwick, R., Decock, J., & Edwards, D. R. (2011). The roles of ADAMTS metalloproteinases in tumorigenesis and metastasis. *Frontiers in Bioscience*, *16*, 1861–1872.

Wang, Y. C., & Ferguson, E. L. (2005). Spatial bistability of dpp-receptor interactions during *Drosophila* dorsal-ventral patterning. *Nature*, *434*(7030), 229–234.

Wei, J., Richbourgh, B., Jia, T., & Liu, C. (2014). ADAMTS-12: A multifaced metalloproteinase in arthritis and inflammation. *Mediators of Inflammation*, *2014*, 649718.

Xie, Y., Gou, Q., Xie, K., Wang, Z., Wang, Y., & Zheng, H. (2016). ADAMTS6 suppresses tumor progression via the ERK signaling pathway and serves as a prognostic marker in human breast cancer. *Oncotarget*, *7*(38), 61273–61283.

How to cite this article: Pham MN, Schuweiler M, Ismat A. The extracellular protease *AdamTS-B* inhibits vein formation in the Drosophila wing. *genesis*. 2018;1–10. https://doi.org/10.1002/dvg.23255